TORNADIC DEBRIS SIGNATURES in TROPICAL CYCLONES

Roger Edwards[1] and Joseph C. Picca
Storm Prediction Center, Norman, OK

1. INTRODUCTION and BACKGROUND

Radar signatures of supercells permit local forecasters to assess, among other threats, a storm's short-fused tornado risk for warning purposes (e.g., Heinselman et al. 2015). Storm behavior and mode also offer insights for all severe-storms forecasters regarding mesoscale environmental conditions. An apparently intense, cyclic supercell would not be showing strong evidence of a debris-lofting tornadic vortex, for example, if atmospheric surroundings were wholly unsuitable for tornadoes—regardless of any contradictory output from environmental objective analyses. Collocated radar features such as reflectivity hooks, strong mesocyclonic rotational velocity magnitude (hereafter V_{rot}) (Smith et al. 2015), anomalies of spectrum width (Spoden et al. 2012), and multiscan temporal continuity of those signatures, have been used to infer sufficient likelihood of a tornado to justify warnings, and even to infer probable intensities of tornadoes (Smith et al. 2015). Moreover, combinations of radar-based, storm-scale characteristics, including convective mode, with mesoscale, diagnostic environmental information (Smith et al. 2012; Thompson et al. 2012; Smith et al. 2015) and short-fused numerical-model guidance, yield beneficial insights into the potential for storms to persist, weaken, or intensify over a nowcasting timespan. As such, clues ascertained from observed radar tendencies are an important part of each Storm Prediction Center (SPC) forecaster's operational toolkit. Such data augment more fundamental, ingredients-based thinking (e.g., Johns and Doswell 1992), in turn, within the broader "forecast funnel" (Snellman 1982) predictive framework.

As part of local warning and SPC tornado-forecasting responsibilities, tropical cyclones (TCs) are a distinct class of mesoscale convective system whose tornadic tendencies have been documented in various ways for nearly a century (e.g., Barbour 1924; Hill et al. 1966; Novlan and Gray 1974; Verbout et al. 2007; Edwards 2012; among many others). Though some weak TC tornadoes are nonsupercellular in nature (Edwards et al. 2012a), the most damaging and great majority of them form in supercells with radar-evident mesocyclones (Edwards et al. 2012b). Radar examinations of TC supercells—both tornadic and nontornadic—have been undertaken since the WSR-88D network was installed in TC-prone regions of the southern and eastern U.S. in the early to middle 1990s (e.g., Spratt et al. 1997; Rao et al. 2005; Agee and Hendricks 2011; Edwards et al. 2012b). Because

TC supercells tend to be shorter-lived, smaller in horizontal and vertical dimensions than their nontropical counterparts, and frequently exhibit messy reflectivity patterns (e.g., Rao et al. 2005; Edwards et al. 2012b), in addition to their common tendency to translate faster, detection of and warning for TC tornadoes generally are more challenging (e.g., Spratt et al. 1997; Schneider and Sharp 2007).

Three crucial post-deployment attachments to the WSR-88D fleet have assisted near-real-time tornado indication, in chronological order:
- So-called "super-resolution" scanning strategy, starting in summer 2008;
- Installation of dual-polarization capabilities (Bringi and Chandrasekar 2001), beginning in November 2010 (NWS 2010); and
- The Supplemental Adaptive Intra-Volume Low-Level Scan (SAILS; Chrisman 2011) method, prior to the 2014 TC season.

The "super-resolution" method involves selective data windowing and oversampling to achieve 250-m range resolution and 0.5° azimuthal spacing (Brown et al. 2002, 2005; Torres and Curtis 2007) of sufficient quality. When interrogating small echoes, and specifically the shallow, narrow mesocyclones that tend to accompany TC supercells, this provides a clear advantage over earlier, lower-resolution output.

A major tool for tornado detection in the era of dual-polarization products is in the spatiotemporal juxtaposition of a mesocyclone with a TDS (tornadic debris signature). A TDS is a pronounced minimum anomaly (generally less than 0.9 out of a theoretical max of 1.0) in copolar cross-correlation coefficient (ρ_{hv}), strongly indicating lofted tornadic debris in a field of meteorological scatterers (Rhyzhkov et al. 2005; WDTB 2015). The TDS is a slightly time-lagged initial diagnostic, since a debris plume only can reach beam height after tornadogenesis. Still, a well-defined TDS is useful for downstream warning decisions, being near-certain affirmation of a tornado within the preceding 5 min or less. TDSs have been related to severity of damage for nontropical, supercellular tornadoes (Bodine et al. 2013). As a subset of a broader work, Edwards et al. (2015) preliminarily investigated ρ_{hv} for TC events at small sample size. They found that TDSs in TCs often stand out well (e.g., archetypes of Figs. 1 and 2, from a case also used herein) due to their presence within nearly homogenous fields of high-ρ_{hv} warm-cloud rain that characterize the TC environment.

---
[1] *Corresponding author address:* Roger Edwards, Storm Prediction Center, National Weather Center, 120 Boren Blvd #2300, Norman, OK 73072; E-mail: roger.edwards@noaa.gov
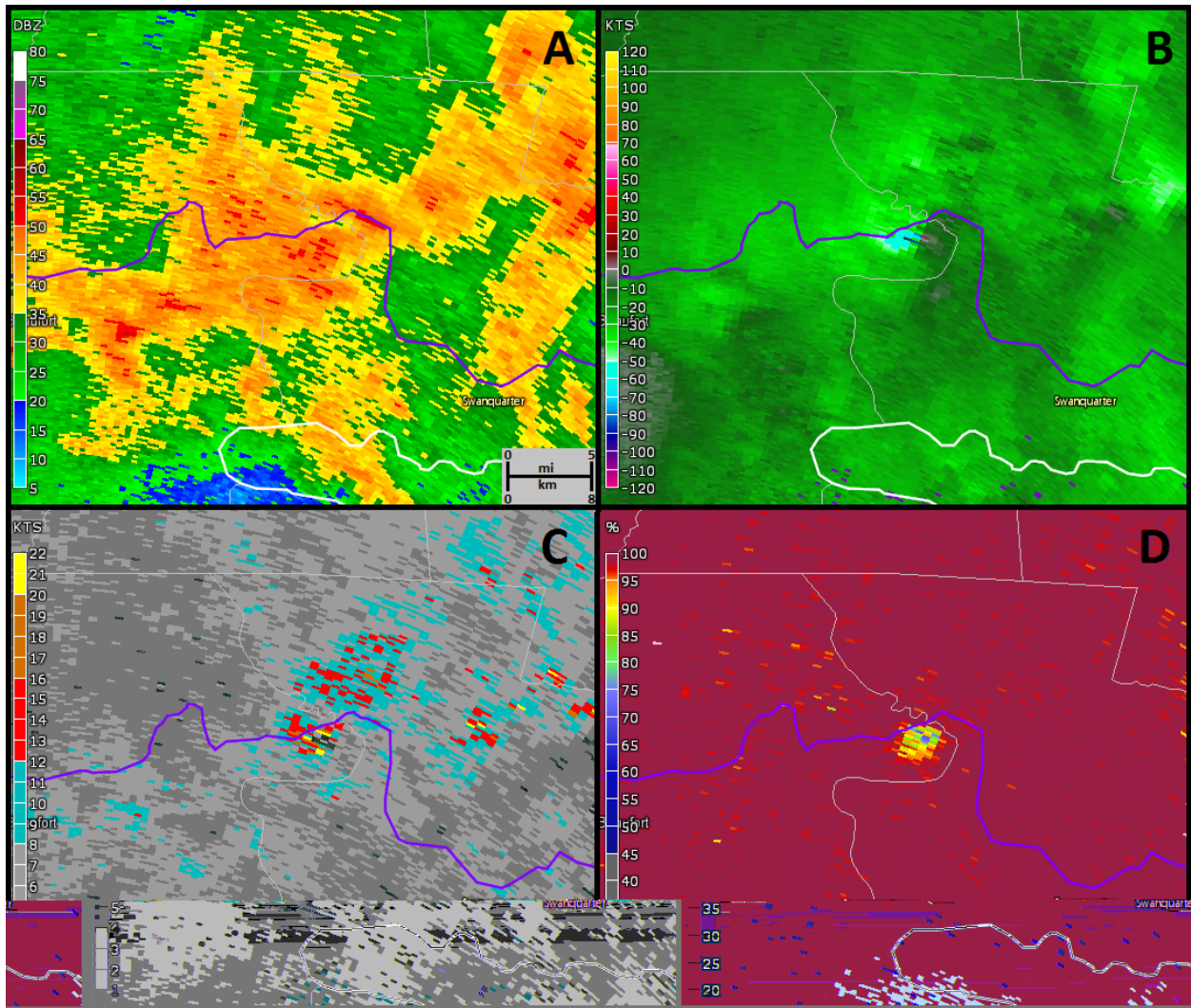
Figure 1: Geographically matching, 0.5° -elevation, four-panel display of products from Morehead City, NC WSR-88D from 0203 UTC 27 August 2011, TC Irene: a) base reflectivity, b) base velocity, c) spectrum width, d) ρ_{HV}. Values and units as shown in scales. Tornado was in extreme eastern Beaufort County, NC at this time, near center of each panel and northeast of the radar, moving generally westward (right–left). Purple curve is U.S. Highway 264. Archetypical TC TDS example from Edwards et al. (2015).
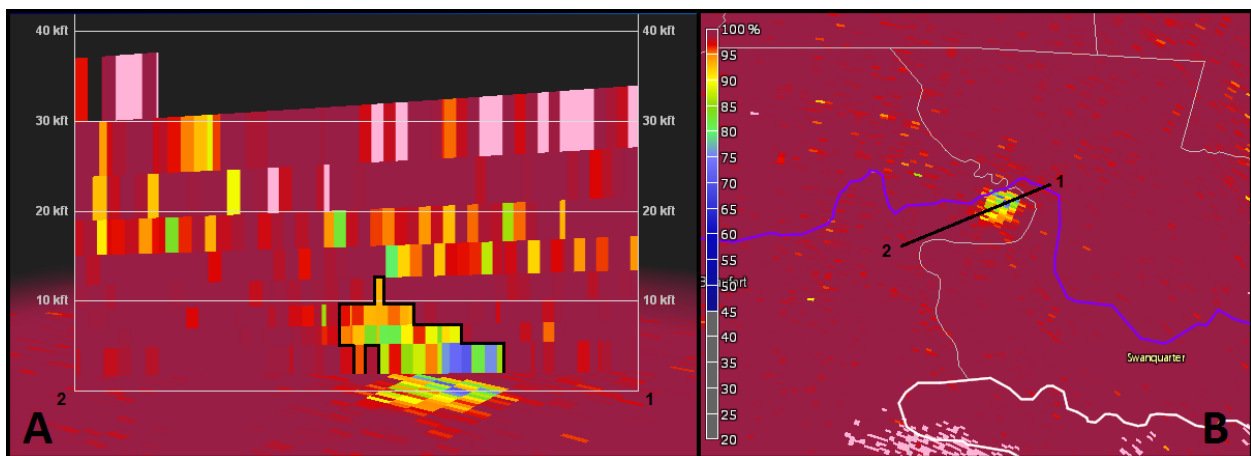

Figure 2: a) Vertical cross section through ρ_{HV} min in Fig. 1d, from 1 to 2 along the black line shown in panel (b). Black outline in (a) represents approximate bounds of the TDS using ρ_{hv} ≤0.9. Adapted from Edwards et al. (2015).
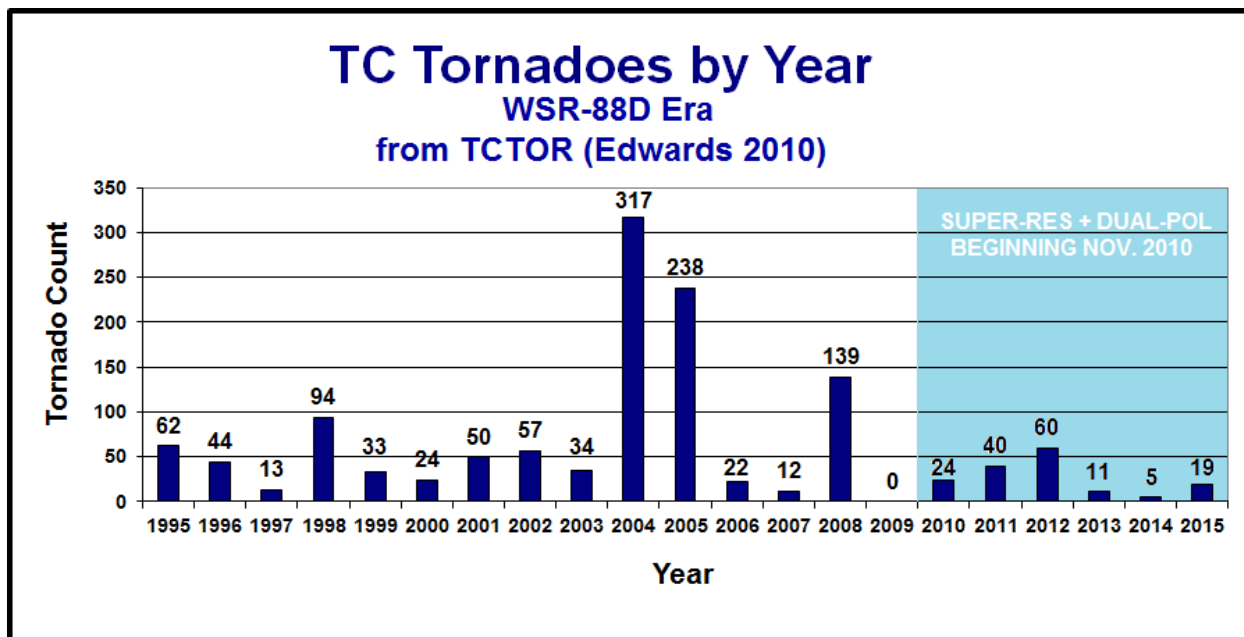
2

<u>Figure 3:</u> Histogram of tornado counts from TCTOR through 2015, with the combined "super-res" and dual-polarization era shaded in light blue. As of this writing, TCTOR is not finalized for 2016.

The third advance, SAILS, involves inserting a "split cut" into two common volume coverage patterns, by mechanically reorienting the transmitted wave back to 0.5° beam tilt halfway through each volume scan. SAILS thus renders two lowest-elevation product sets per ~5–6 min and slightly increases full-scan time. In combination with "super-resolution" and dual-polarization output, SAILS is especially advantageous for surveillance of small, fast-moving, rapidly evolving supercells, as are common in TCs. Starting in May 2015, even more frequent scan splits back to 0.5° have been field-tested on a subset of the WSR-88D radar network as a part of the Multiple Elevation Scan Option (MESO) SAILS (Chrisman 2014). Since they include 0.5° ρ_{hv}, SAILS and MESO-SAILS offer sooner TDS detection at higher temporal sampling intervals. As such, and despite the relative dearth of U.S. tornadic TCs since dual-polarized radar upgrades (Fig. 3, above), opportunities are growing for analyses of these events.

This preliminary work extends the TDS data discussed as a 23-sample tornadic subset of Edwards et al. (2015)—a study that also encompassed other radar attributes and environmental characteristics of 112 supercellular tornadoes.   Here, we focus exclusively on TC TDS events. Radar imagery is examined and classified for detectable U.S. TDSs in TCs so far, most of which were accompanied by tornado reports. Section 2 describes data used and analyses performed.   Section 3 offers preliminary results, and section 4 contains conclusions and discussion.

2. DATA, METHODS and EXAMPLES

a. Tornado and radar data

The SPC TC tornado dataset (TCTOR; documentary details in in Edwards 2010) was queried for the 2010–2015 period encompassing the WSR-88D dual-polarization era, which has corresponded to a relative lull in TC tornadoes (Fig. 3). To boost sampling, preliminary 2016 tornado reports from local NWS storm reports were used as well, pending final *Storm Data* and TCTOR entry. For each known tornadic TC in the contiguous U.S. in that period, radar data from WSR-88D units with dual-polarization capability were downloaded from NCEI, then displayed and examined in Gibson Ridge GRLevel2® software used to produce radar-image figures herein. Priority was given to tornadic supercells; however, the process of examining data for those fortuitously revealed supercellular TDSs unaccompanied by tornado reports.

b. Echo and tornado characteristics

Convective mode (i.e., discrete, clustered, embedded in a line, etc.) and V_{rot}), each following the methods of Smith et al. (2012), and echo tops (ET) were determined for each supercell during the period of a TDS. After convective mode was assigned to each echo at tornadogenesis time (including adjusted times where necessary), maximum V_{rot} was assessed during tornadic lifecycle. As done in Edwards et al. (2012b, e.g., their Fig. 8), a peak 20-dBZ echo height above radar level (ARL) was estimated for the full volume scan closest to adjusted tornado time for each event, using the nearest WSR-88D capable of sampling full storm depth.   This technique included the use of range-height indicator (RHI)-style cross-sections, pivoted and slid horizontally in both *x* and *y* planes for optimal sampling. However, instead of

3

rounding to the nearest 1000 ft (305 m) as in that study, we continued the practice from Edwards et al. (2015) of linear interpolation between elevation angles that straddled the top of the 20-dBZ echo intensity. This procedure is consistent with the recent RHI-based ET-determination practice advocated by Lakshmanan et al. (2013). Our reflectivity threshold was maintained at 20 dBZ because:

- The 20 dBZ criteria for tropical convection was established by Cifelli et al. (2007);
- Conveniently, 20 dBZ the closest RHI contour value in GRLevel2[TM] software to the 18-dBZ midlatitude ET threshold shown by Lakshmanan et al. (2013).

Damage ratings also were examined for tornadic events. Twenty (56%) were associated with EF0 damage, 15 (42%) were EF1, and one was EF2 on the enhanced Fujita (Edwards et al. 2013) scale. Unlike in Smith et al. (2012), no filtering was done for EF-rating and proximity, given the small sample of TC events compared to those elsewhere nationwide.

c. TDS documentation

The minimum ρ_{hv} (collocated with both a mesocyclone and spectrum-width[2] anomaly) was recorded for each case. As no TCs in 2010 produced tornadoes within range of dual-polarization radars, the first case was in TC Irene in eastern North Carolina, 0158 UTC 27 August 2011. As in NWS Warning Decision Training Division (2015) guidelines, our threshold ρ_{hv} values was ≤0.95 and/or a pronounced local minimum juxtaposed with reflectivity of 20 dBZ. If a TDS was found in radar imagery, it was used, regardless of the existence of another tornado in spatiotemporal proximity, or even the existence of a tornado report with the TDS. In fact, seven TDSs documented so far either occurred with no corresponding tornado report, or are from 2016 and lacked a preliminary tornado designation in local storm reports. These will be called "no-report" hereafter, acknowledging the physical possibility (likelihood?) of an unreported tornado having caused the TDS. An example of a no-report TDS is shown in Figs. 4 and 5.

So far, 36 TDSs were associated with tornado reports. These included one tornado heretofore not in ONETOR or the parent SPC master database, but found by happenstance in a *Storm Data* search for more information on a separate, nearby event. That missing tornado, which has been added to TCTOR and submitted for addition to the parent SPC database, was at 1836 UTC 31 August 2012, in Jersey County, IL. Two TDSs, the first beginning 1811 UTC 1 September 2012 in Stark County, IL, and the second on 19 June 2015 in Richland County, IL, were conterminous with two tornadoes apiece. Given the uncertainty of determining when the debris from the second tornado infiltrated the preexisting TDS, to

---

[2] Although values of spectrum width were not recorded for this study, imagery thereof, and of other base moments, aided in finding and tracking tornadic echoes; Spoden et al. (2012) offers discussion on this and other utilities of spectrum width.

what magnitude, and for how long, their TDS characteristics will be associated with the first tornado for analytic purposes. Another tornado—Collier County, FL, 24 June 2012, 1600 UTC—produced a ρ_{hv} plume that penetrated a pre-existing, weakening TDS in the same storm, but with visually very distinctive pattern strongly suggesting a new TDS.

All TDSs were within 130 mi (209 km) of radar sites, because of beam-sampling considerations (height and resolution limitations) at longer distances. Only five (12%) of TDSs were identifiable at distances >100 nm (161 km). Tornadic events were gathered only from supercells, based on the storm-classification methods employed by Smith et al. (2012). Nonsupercell TC tornadoes (Edwards et al. 2012a) that were sampled did not exhibit TDSs; and no-report TDSs have not been found yet from nonsupercellular echoes. This does not preclude such events, of course, and this preliminary analysis almost certainly has not yet captured all TDSs ever detected in tropical cyclones to this writing. Tornado and TDS duration also were recorded. When TDSs existed for one volume scan, the conservatively assigned duration was 1 min, acknowledging that debris probably was aloft for either longer within the scan time, or undetected at other scans.

Consistent with the Lakshmanan et al. (2013) echo-top procedure, TDS height was assigned to the highest beam level of the ρ_{hv} plume apparent in RHI cross sections that was vertically continuous with the underlying TDS. If only the lowest beam elevation contained a qualifying ρ_{HV} minimum, that beam's height (ARL) was used. For strongly tilted debris columns where beam-resolution limitations imparted *horizontal* displacements in threshold ρ_{hv} values from one *vertical* beam level to the next (e.g., Fig. 5a), visual inspection determined subjectively if the debris column was coherent along its steep axis. If such visual interpretation indicated that the debris plume extended above the highest embedded gate of ρ_{hv} ≤0.95, we nonetheless kept the latter value as the limiting threshold for TDS height, to be consistent with the previously defined bounding value of a TDS in beam-planar (quasi-horizontal) usage.

d. Error sources in tornado and TDS data

As in Smith et al. (2012) and Edwards et al. (2015), some original tornado-data entry errors needed repair. Tornado times were adjusted when radar evidence compelled. For example, when no radar echo existed overhead at the *Storm Data* genesis time, the actual time used was adjusted to better match the passage of the mesocyclone. Six cases necessitated such correction, including one where the recorded tornado time was one hour off, apparently due to incorrect entry of the time zone. Four other of those events were time-corrected to one volume scan prior to the start of the TDS (i.e., the TDS began at or downshear from the given tornado location prior to the stated *Storm Data* tornado time, which was adjusted). In total, seven TDSs began before stated tornado time and/or upshear of the tornado location; TDSs beginning upshear from the *Storm Data* tornadogenesis point (e.g., Figs. 6 and 7)
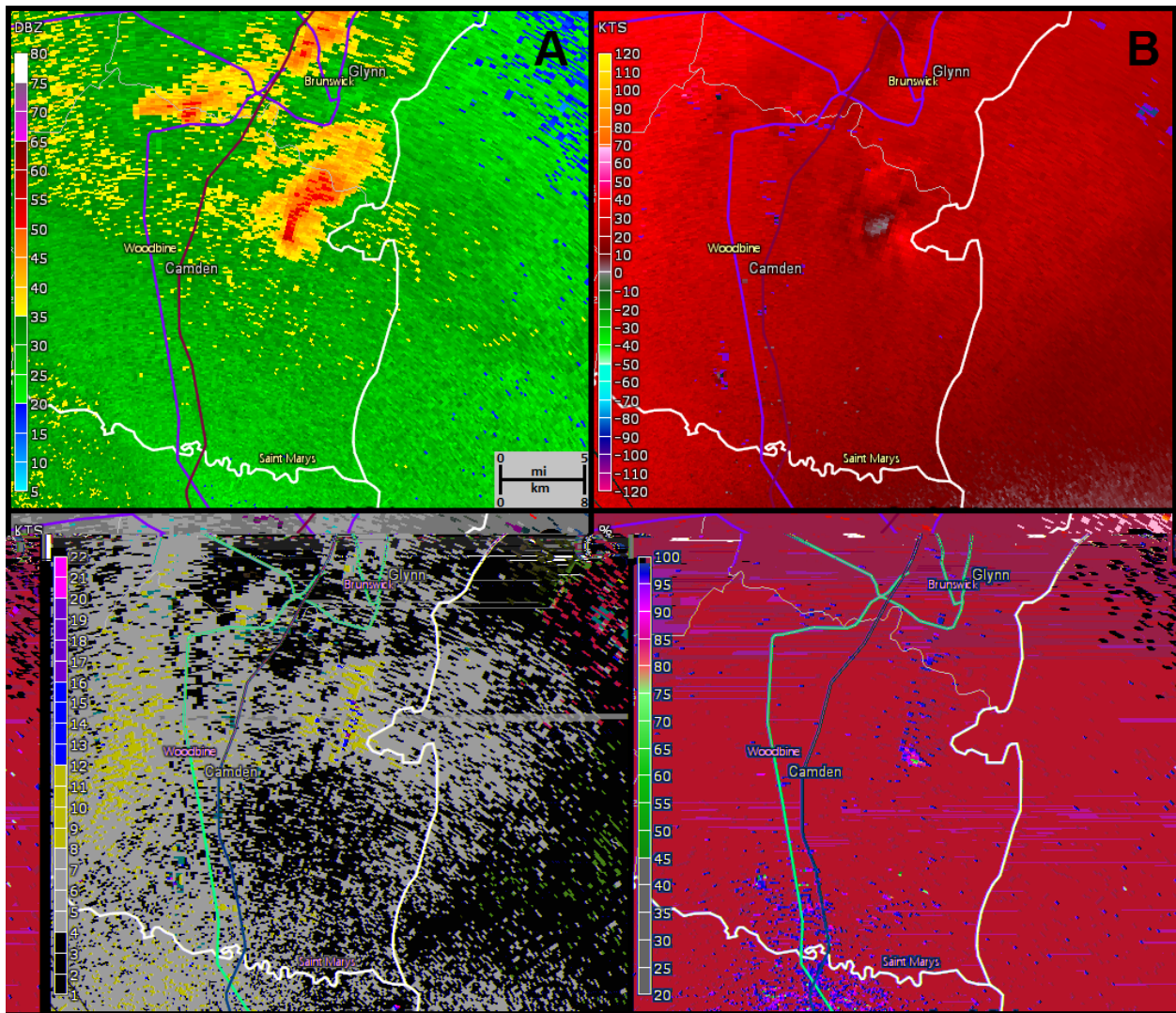
Figure 4: As in Fig. 1, but for the Jacksonville, FL WSR-88D, 0421 UTC 2 September 2016, TC Hermine. TDS was over a remote, sparsely inhabited area of eastern Camden County, GA, north-northeast of the radar, and was not associated with either a reported tornado, structural damage, or clearly tornadic vegetative damage distinguishable from that of the TC itself (A. C. Sandrik, personal communication). Red curve is Interstate 95.
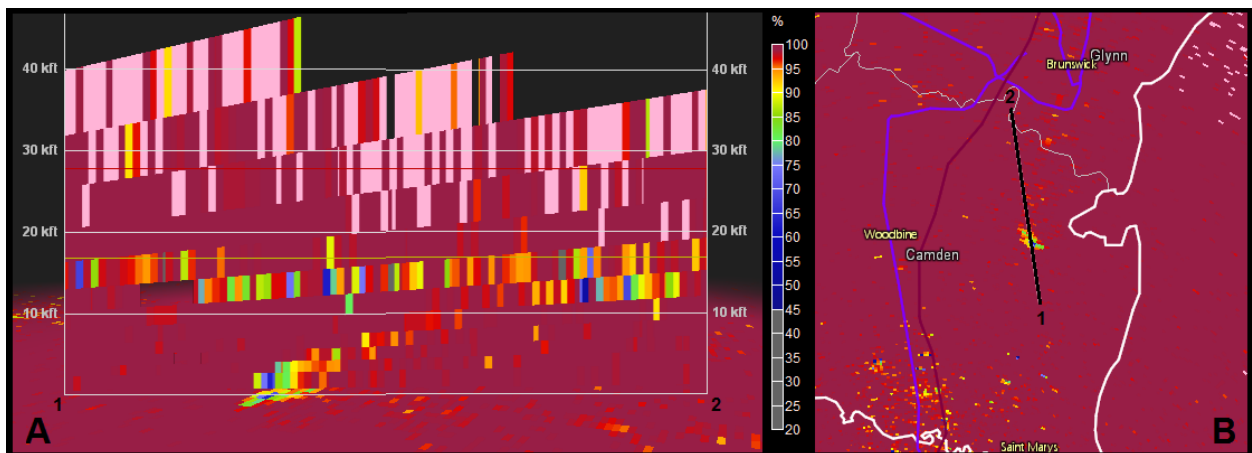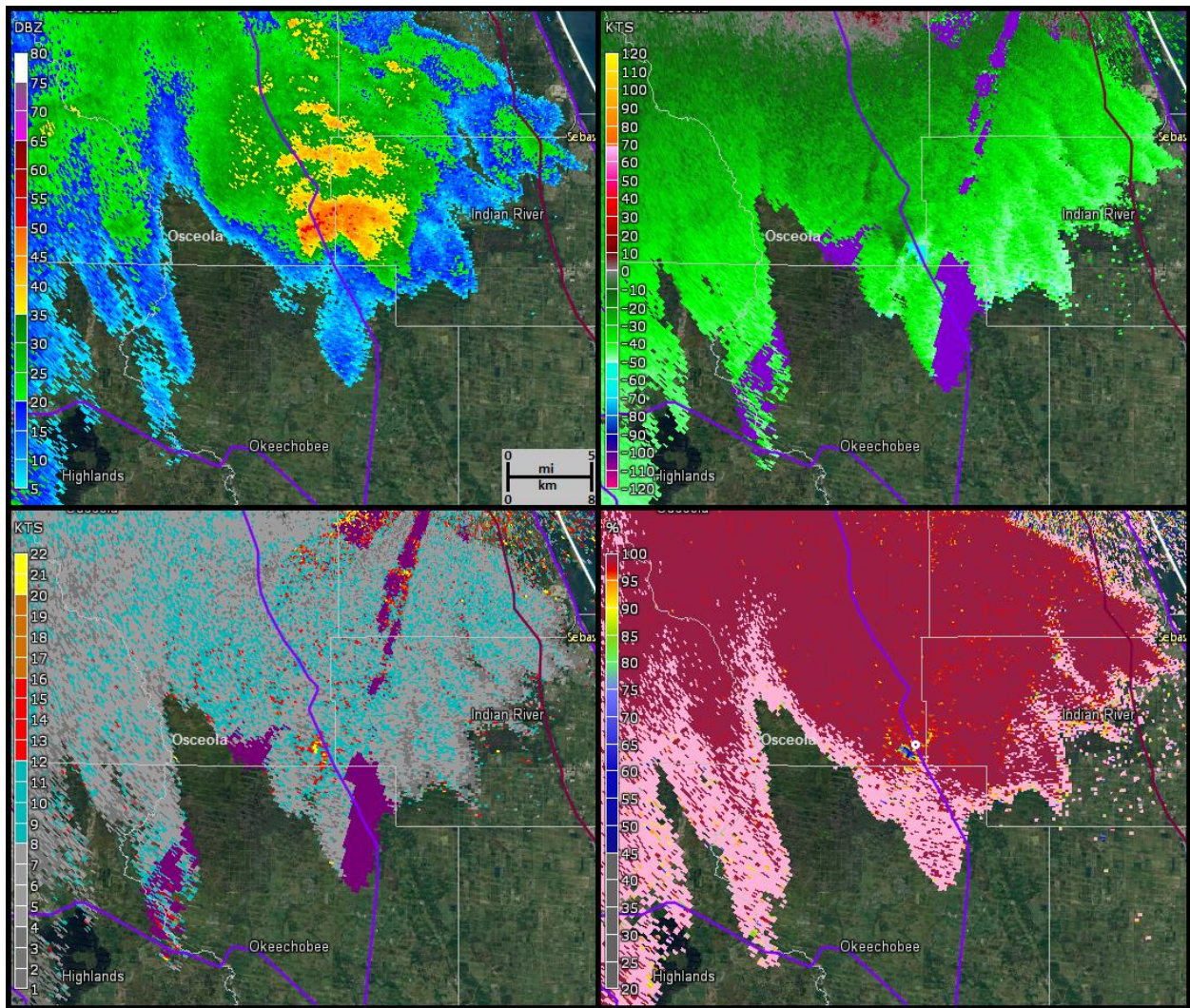

Figure 5: As in Fig. 2, but for the Jacksonville case shown above in Fig. 4.

Figure 6: As in Fig. 1, but for the Melbourne, FL WSR-88D, 0153 UTC 25 June 2012, TC Debby. Supercell was moving northward. TDS was located south of and 2 min before the tornado report (white circle) in southeastern Osceola County, along U.S. 441 (purple curve), southwest of the radar. The TDS was initially evident but more poorly defined one volume scan earlier at 0148 UTC, and located even farther south in extreme northern Okeechobee County (not shown).
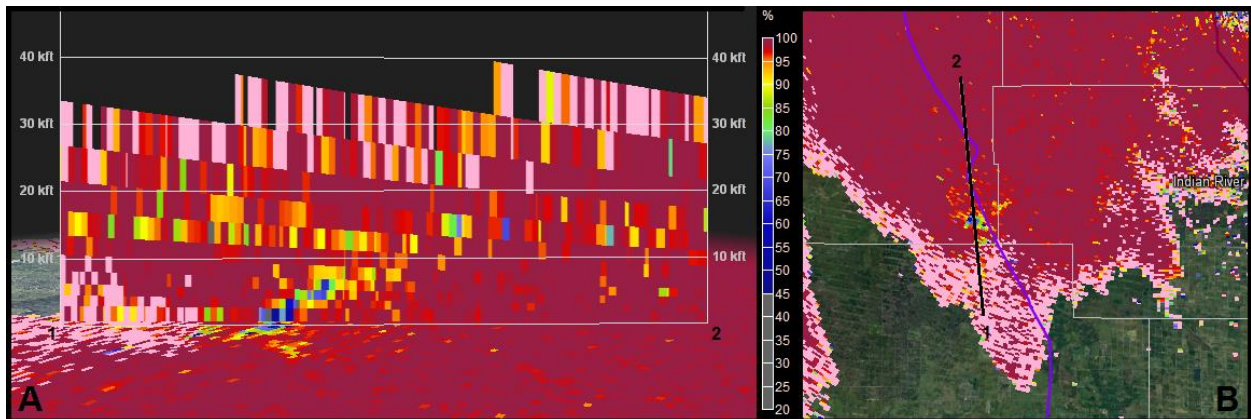
Figure 7: As in Fig. 2, but for the Melbourne case shown in Fig. 4 in the 0154 UTC SAILS scan (1 min before tornado report).
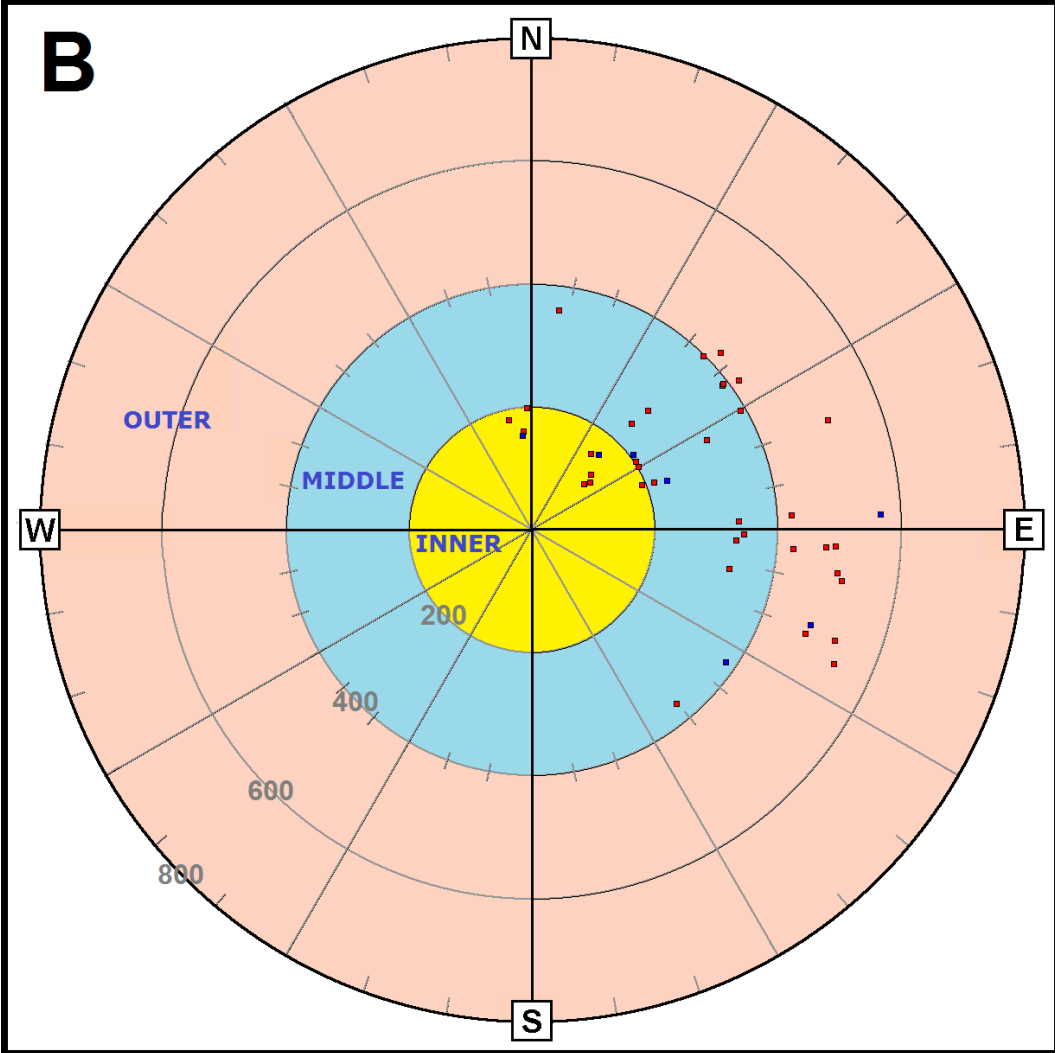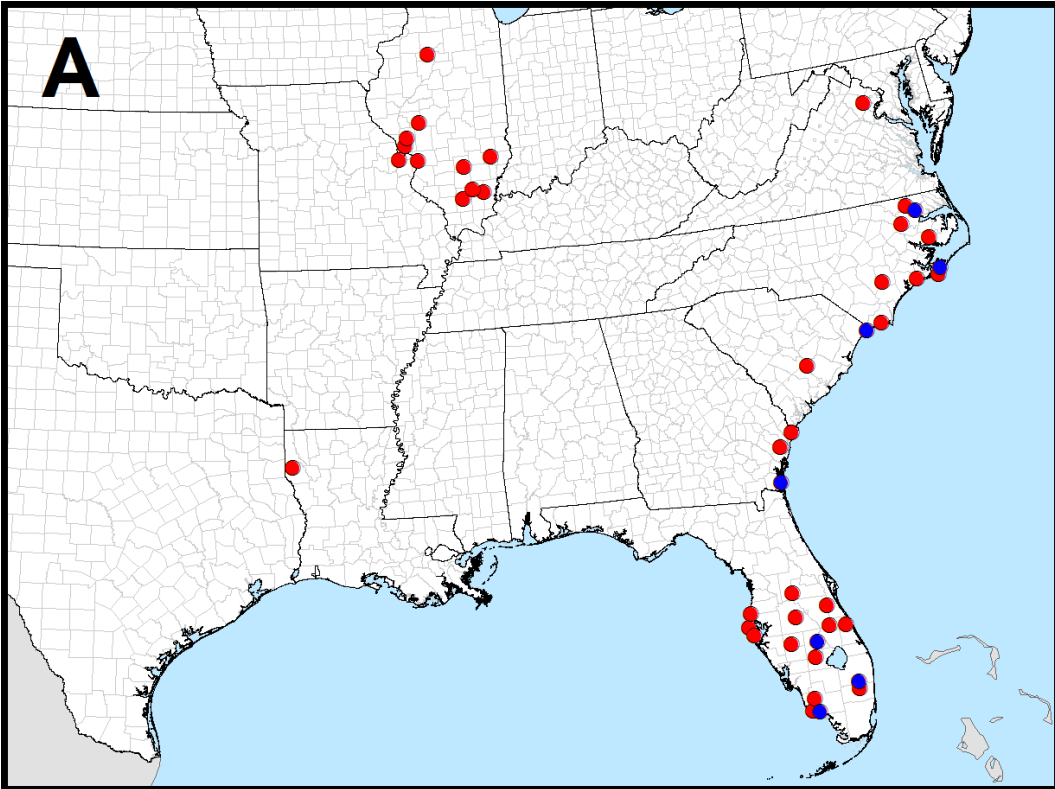
A

B

N

OUTER

MIDDLE

W

INNER

200

400

600

800

S

E

were not assigned a specific new starting location due to uncertainty, including lack of available survey evidence. One TDS began after recorded tornado time but upshear of its location, and similarly could not be location-corrected due to uncertainty. Another case was location-corrected due to an erroneous transposition of tenths and hundredths digits in its Storm Data latitude entry that initially placed the tornado outside the causative supercell. Simply flipping those digits placed the tornado directly within the radar-evident mesocyclone at the recorded time.

Given the limited sample size of the dataset, the multivariate discrepancies in recorded tornado characteristics compared to some TDSs, and the uncertainties inherent to estimating unreported tornadogenesis prior to a TDS, our initial plans to overlay tornado and TDS timelines are unfulfilled for now. Still, their respective known durations will be examined for each event and in bulk (below). Tornadoes with identical start and end times in Storm Data were assigned a 1-min lifespan. No explicitly zero-magnitude recorded path lengths were found, though one event had the same starting and ending latitude/longitude points recorded.

Figure 8 shows the distribution of both tornadic and no-report TDSs, with respect to U.S. geography and to the center of each TC at tornado time. The latter was calculated and mapped using the interpolated hurricane best-track dataset and spherical geometry, as described in detail in Edwards (2010). Neither represents a climatological distribution of TC tornadoes, because of the relatively small sample size of our TDS data and the fortuitous nature of radar positioning with respect to those events that have been detected. Still, the polar distribution of TDSs fits well within those of TC tornado climatologies for the WSR-88D era shown in Edwards (2010; 2012). Curiously, the TDS data so far are missing events 400–800 km southeast through south of TC center. Beyond chance, or simple lack of data due to limited sampling, any potential physical explanation of this artifact would be overly speculative at this time, and outside the scope of this work.

3. RESULTS and CONCLUSIONS

a. TDS characteristics

TDS events were analyzed both in bulk and just for tornadic events. Since only seven no-report TDSs were available for this examination, not much can be stated outside of means. No-report TDSs averaged slightly weaker (i.e., higher) minimum ρ_{HV} values vs. tornadic (55.7 vs. 60.2), identical duration (12.7 min), somewhat stronger V_{rot} (37.4 kt or 19.2 m s^{-1} vs. 31.6 kt or 16.2 m s^{-1}), slightly higher absolute height (2448 vs. 3308 m ARL), but slightly lower relative depth within echoes (26% vs. 29% of ET). Without a more robust sampling of no-report events, and with such small differences in preliminary means, there is insufficient data to state, with reasonable certainty,

any characteristic distinctions between tornadic and no-report TDSs.

Preliminary TDS-related data for the whole dataset appear in Table 1. These findings reinforce earlier, smaller-sample-size information in Edwards et al. (2015) that TDSs occupied highly variable proportions of the echo depths, as measured by TDS height percent of ET. The lowest ET-relative TDS was just 2% (0.5° scan near the radar, 250 m ARL); the other extreme attained 84% of a 6.4-km ET. A different lowest-beam TDS reached 3% of ET with a TDS height 263 m ARL. From an absolute-depth framework, the highest TDS was 9.2 km ARL, 69% of its parent ET. TDSs appeared as far as 206 km from the radar, though only three cases were evident at >175 km range. In terms of V_{rot}, considerable variation also was evident. Rotational velocity V_{rot} was highly variable, with values from 12–60 kt (6–30 m s^{-1}). Discussion on how TC TDS V_{rot} compares with other tornadoes appears in the next subsection.

Table 1: Summary of TDS characteristics from the entire TDS dataset: lowest columnar ρ_{hv} value, range from radar (km), height ARL (m), percentage of associated ET, and V_{rot} (kt).

TDS	ρ_{hv}	Range (km)	Hgt (m)	% ET	V_{rot} (kt)
Avg.	.56	91	3331	29	32.5
Median	.60	86	2870	22	32.1
Max	.895	206	9166	84	59.7
Min	.208	19	250	02	12.2

b. Comparisons with non-TDS tornadoes

Edwards et al. (2015) hypothesized that TC TDS have lower Vrot than most midlatitude (nontropical) events, and a higher damage rating, greater V_{rot} and loftier ET, versus non-TDS tornado reports in TCTOR. We additionally hypothesized that path lengths and widths—and in combination with ratings, the destruction potential index (DPI; Thompson and Vescio 1998)—should be larger for TDS-producing tornadoes.

When comparing only the tornadic TDSs to the expansive dataset of tornadic, mostly nontropical, supercellular V_{rot} values from Smith et al. (2015), the mixture of mostly EF0 and EF1 events from our data fit closely with their distribution accompanying EF0 tornadoes nationwide (Fig. 9). Our distribution was slightly lower at all conventional percentile markers for the boxplots except for a match at the 10th. Because our sample size overall is two orders of magnitude smaller, caution should be taken against interpreting our preliminary findings as representative of all possibilities for V_{rot} in the TC setting, with or without TDSs. Still, given the weak and small nature of TC tornadoes in general, these findings were not surprising.

0.5° PEAK ROTATIONAL VELOCITY (kt)
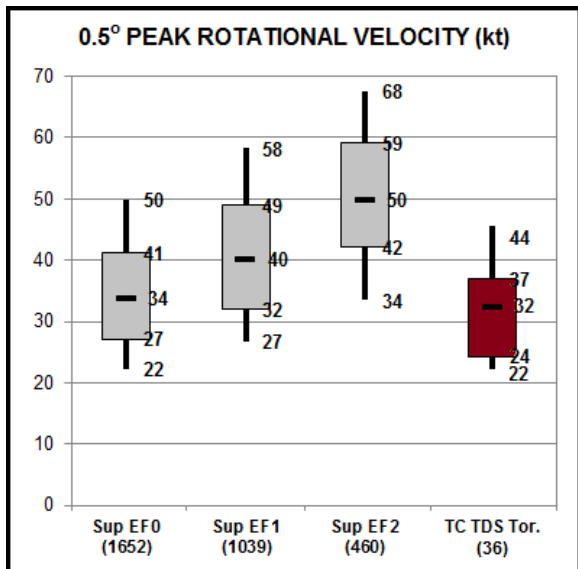
Figure 9: Box plots of all tornadic TC TDS V_{rot} distributions (dark red, right) compared to those from Smith et al. (2015) tornadic supercells by EF rating (gray), in kt. Boxes represent 25th and 75th percentiles; whiskers extend to 10th and 90th percentiles, and bars are medians. Sample sizes in parentheses.

Path attributes for the 36 tornadoes with TDSs were compared to the 103 without TDSs during the same 2011–2015 timespan, following the hypothesis that TDS-producing tornadoes would be more substantial. The same sampling timespan was chosen for more compatibility of both tornadic TC regimes and event sample size (only an order of magnitude difference, versus two against the entire TCTOR dataset). The path characteristics available in TCTOR were length, width and EF-scale (Edwards et al. 2013) damage rating. All tornadoes were rated EF0, EF1 or EF2, with only one EF2 event in the TDS sample (as noted in section 1) and three EF2s in the "no TDS" group. This tendency toward weak damage rating, with a dearth (in this case complete absence) of >EF2 events, is consistent with the climatological nature of TC tornadoes as a whole (Edwards 2012). Sixteen (44%) of tornadoes with TDSs were rated ≥EF1, compared to 25 (24%) of those lacking a TDS. Damage rating also is incorporated with path length and width into the DPI, whose relative distributions were analyzed.

Path lengths necessarily constrained to near zero on the low end of the distributions, but were offset by nearly a quartile in favor of tornadoes with TDSs versus those without (Fig. 10). Path widths, EF rating and the combined index of DPI (not shown) similarly constrain near zero, but were more subtly shifted toward TDS events on the high side of the distribution than path length.

These findings appear to affirm our hypothesis that TC tornadoes with TDSs are more substantial overall than those without, all other aspects considered. Importantly, tornadoes may lack TDSs due to other factors, including:

- Distance from radar and related poor spatial beam sampling, especially given the tendency for smaller mesocyclones in the horizontal and vertical in TCs (Edwards 2012);
- Poor temporal beam sampling due to tornadic brevity, especially before the SAILS era;
- Obscuration of a TDS by lower ρ_{hv} from melting hydrometeors, non-uniform beamfilling, etc. (not common in the TC setting); and
- Lack of dual-polarization capability of nearby radar(s).

The latter, though not a problem from the 2013 TC season onward, was common in 2011 and 2012, when many WSR-88D units near the Gulf and Atlantic coasts had not been upgraded yet. As such, *the "no TDS" dataset probably includes some tornadoes capable of producing TDSs*. This makes the disparity shown in Fig. 10 even more remarkable.

PATH LENGTH 2011–2015
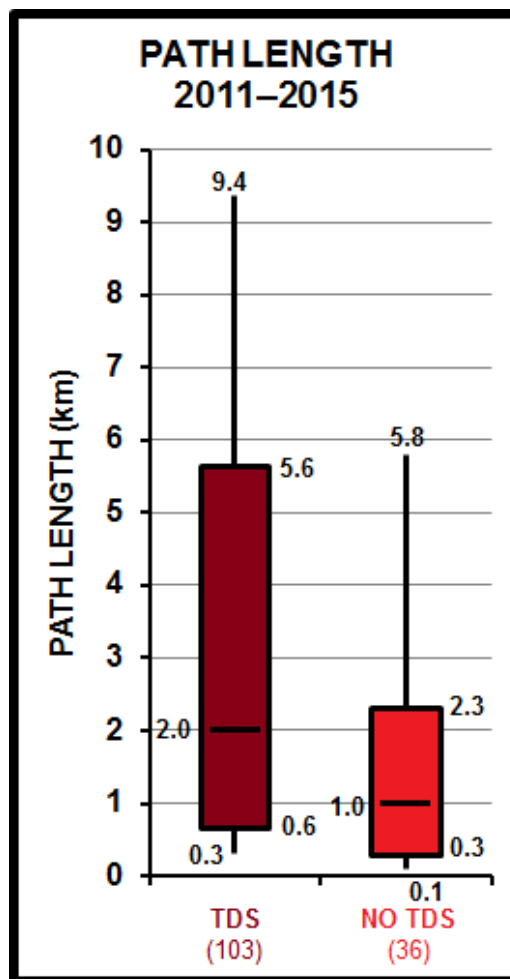
Figure 10: Box plots of path length (km) for TC tornadoes with TDSs (left, dark red) and without (right, red) in the 2011–2015 subset of TCTOR. Boxes extend to 25th and 75th percentiles with values on right corners. Medians denoted by horizontal bars and values at left. Whiskers extend to 10th and 90th percentiles with values given. Sample sizes appear in parentheses at bottom.

4. AREAS for ADDITONAL STUDY

Sample size and quality are substantial concerns with any analyses of tornado data, as discussed by Doswell (2007). These concerns certainly apply to such a narrowly specialized subset of data as tornadoes with TDSs in TCs, even when performing the sort of data-quality and meteorological controls described above and in the TCTOR documentation (Edwards 2010). As for quantity, the only solution from here onward will be provided by the atmosphere—namely, more TC tornadoes within TDS-detection ranges of WSR-88Ds. A slightly above-average season for TC tornadoes, while undesirable from an impact-threat perspective, may double the sample size we have been able to accumulate in the first six years of the dual-polarization era.

Given that all WSR-88Ds now are equipped with dual polarization, the lack of coexistence of tornado reports with some TDSs likely will remain a troubling issue in radar meteorology, especially in TCs. Storm spotters in TCs face a daunting challenge in the tornadoes' typically small size, short duration, often poor visual definition, and obscuration by rain, trees, low clouds, and/or darkness (Edwards 2012)—not to mention the ambient hazards of wind and flooding offered by the TC at large. The event in Fig. 3 exemplifies a further difficulty in confirming an apparently no-report TDS in remote areas, having occurred over terrain characterized by marshes with occasional stands of pine trees. A survey along the few area roads by local emergency management found no evidence of outstanding damage aside from that which could be associated with the TC itself (A. C. Sandrik, personal communication). TC damage can mask that from weak tornadoes, though improved storm-survey techniques and the presence of other Doppler radar signatures have been associated with markedly improved TC-tornado documentation in the WSR-88D era (Edwards 2012).

TDSs can offer compelling additional evidence of the likelihood of a tornado. The question is: how compelling? To that end, with sufficiently large datasets of TDSs accompanying weak tornadoes, perhaps a probabilistic assessment of the presence of a tornado can be assigned based on the characteristics of the "no-report" TDS, and recorded accordingly. While not a binary (yes or no) confirmation, a high likelihood of a tornado's presence based on a TDS recognizes that: 1) probability is the language of uncertainty, and 2) the high probability of a tornado's existence in absence of *Storm Data* reports (ground confirmation) still may suffice for many radar-research and risk-analysis purposes. How high? That may be calibrated to the strength, depth, and duration of a "no-report" TDS. A much larger sample than available here likely would be needed to develop such a probabilistic algorithm.

A secondary concern for this study (due to our ability to perform manual investigations and corrections in a small sample), but one vital to tornadic data mining as a whole, is the presence of many types of errors in the data. To what extent do our error discoveries, along with those of Smith et al.

(2012) and Edwards et al. (2012a,b) represent a microcosm of the national dataset? From assorted common time errors (e.g., bad time-zone entries, times devoid of echoes) to transposed latitude/longitude digits, other typos in data logging, and *nominal tornadogenesis locations and times occurring after their TDSs begin*, the prospect of a dataset riddled with an unknown quantity of tornado time and location errors is troubling. Manual interrogation of tens of thousands of tornado reports for correspondence with radar echoes is not practical. Reports can be compared with mesocyclone signatures or TDSs in automated ways; but that process would neglect nonsupercell tornadoes, legitimate tornadoes without TDSs (e.g., discussion section 3f), and non-mesocyclonic tornadoes that occur in other parts of supercells. For now, there appears to be no ready solution to this quandary for bulk analyses of nationwide tornado datasets.

For TC purposes, use of only significant events is not practical for maintaining robust sample size, as it would exclude around 93% of all TC tornadoes (Edwards 2012). Paradigm shifts in warning and verification practices coincident with the installation of the WSR-88D network, as well as damage-rating subjectivities and inconsistencies (e.g., Doswell and Burgess 1988; Edwards et al. 2013) also are likely sources of TC tornado data error (Edwards 2012) and may extend to the national dataset as a whole.

Further analysis of samples within this dataset (as well as future samples yet to be added) may offer an avenue for enhanced training of warning forecasters. For example, comparisons of TC TDS characteristics (and their correlation with various tornado metrics) with those of non-TC TDSs may reveal important differences that could be exploited to improve warning-decision training.

One topic of further exploration entails comparisons of non-TC and TC TDSs via model scattering simulations. For example, if we assume two hydrometeor distributions—one typical of continental precipitation (characterized by melting ice and larger drops) and another typical of tropical precipitation (characterized by smaller drops and a lower concentration of ice), identical distributions of debris mixed with each distribution of reflectors would result in varying depressions in CC values. Due to the lower backscattered signal of the tropical rainfall, debris would have a larger relative contribution to the total backscattered signal, thereby further reducing CC in the range gate. Model support of this hypothesis could enhance understanding of why TC TDSs often appear more prominently with weak tornadoes. Subsequently, future operational work could incorporate these expected TDS differences between tropical and nontropical environments into warning-decision training.

Smith plotted the planar map in Fig. 8a. John Hart wrote the radial-plotting script for Fig. 8b. The SPC Science Support Branch maintains the software and hardware used for our analyses.

REFERENCES

Agee, E. M., and A. Hendricks, 2011: An assessment of the climatology of Florida hurricane-induced tornadoes (HITs): Technology versus meteorology. *J. Climate*, **24**, 5218–5222.

Barbour, G. B., 1924: Waterspout and tornado within a typhoon area. *Mon. Wea. Rev.*, **52**, 106–107.

Bodine, D. J., M. R. Kumjian, R. D. Palmer, P. L. Heinselman, and A. V. Ryzhkov, 2013: Tornado damage estimation using polarimetric radar. *Wea. Forecasting*, **28**, 139–158.

Bringi, V. N., and V. Chandrasekar, 2001: *Polarimetric Doppler Weather Radar: Principles and Applications*. Cambridge University Press, 636 pp.

Brown, R. A., V. T. Wood, and D. Sirmans, 2002: Improved tornado detection using simulated and actual WSR-88D data with enhanced resolution. *J. Atmos. Oceanic Technol.*, **19**, 1759–1771.

——, B. A. Flickinger, E. Forren, D. M. Schultz, D. Sirmans, P. L. Spencer, V. T. Wood, and C. L. Ziegler, 2005: Improved detection of severe storms using experimental fine-resolution WSR-88D measurements. *Wea. Forecasting*, **20**, 3–14. Chrisman, J. N., 2011: Supplemental Adaptive Intra-Volume Low-Level Scan (SAILS), 13 pp. [Available online at http://www.roc.noaa.gov/wsr88d/PublicDocs/NewTechnology/SAILS_Initial_Presentation_Sep_2011.pdf.]

——, 2014: Multiple Elevation Scan Option for SAILS (MESO-SAILS), 27 pp. [Available online at http://www.roc.noaa.gov/wsr88d/PublicDocs/NewTechnology/MESO-SAILS_Description_Briefing_Jan_2014.pdf.]

Doswell, C. A. III, 2007: Small sample size and data quality issues illustrated using tornado occurrence data. *Electronic J. Severe Storms Meteor.*, **2** (5), 1–16.

——, and D. W. Burgess, 1988: On some issues of United States tornado climatology. *Mon. Wea. Rev.*, **116**, 495–501.

Edwards, R., 2010: Tropical cyclone tornado records for the modernized National Weather Service era. Preprints, *25th Conf. on Severe Local Storms*, Denver, CO, Amer. Meteor. Soc., P2.7.

——, 2012: Tropical cyclone tornadoes: A review of knowledge in research and prediction. *Electronic J. Severe Storms Meteor.*, **7** (6), 1–61.

——, A. R. Dean, R. L. Thompson and B. T. Smith, 2012a: Nonsupercell tropical cyclone tornadoes: Documentation, classification and uncertainties. Preprints, *26th Conf. on Severe Local Storms*, Nashville TN, Amer. Meteor. Soc., 9.6.

——, ——, ——, and ——, 2012b: Convective modes for significant severe thunderstorms in the contiguous United States. Part III: Tropical cyclone tornadoes. *Wea. Forecasting*, **27**, 1114–1135.

——, J. G. LaDue, J. T. Ferree, K. Scharfenberg, C. Maier, and W. L. Coulbourne, 2013: Tornado intensity estimation: Past, present, and future. *Bull. Amer. Meteor. Soc.*, **94**, 641–653.

——, B. T. Smith, R. L. Thompson and A. R. Dean, 2015: Analyses of radar rotational velocities and environmental parameters for tornadic supercells in tropical cyclones. Preprints, *37th Conf. on Radar Meteorology*, Norman, OK, 5A.3.

Heinselman, P., D. S. Ladue, D. M. Kingfield, and R. Hoffman, 2015: Tornado warning decisions using phased-array radar data. *Wea. Forecasting*, **30**, 57–78.

Hill, E. L., W. Malkin and W. A. Schulz Jr., 1966: Tornadoes associated with cyclones of tropical origin—practical features. *J. Appl. Meteor.*, **5**, 745–763.

Johns, R. H., and C. A. Doswell III, 1992: Severe local storms forecasting. *Wea. Forecasting*, **7**, 588–612.

Lakshmanan, V., K. Hondl, C. K. Potvin, and D. Priegnitz, 2013: An improved method for estimating radar echo-top height. *Wea. Forecasting*, **28**, 481–488.

National Weather Service (NWS), 2010: Technical implementation notice 10-23. [Available online at http://www.roc.noaa.gov/WSR88D/PublicDocs/DualPol/tin_10-23dual_pol88d.pdf.]

Novlan, D. J., and W. M. Gray, 1974: Hurricane-spawned tornadoes. *Mon Wea Rev.*, **102**, 476–488.

NWS Warning Decision Training Division, cited 2015: Dual-pol radar applications: Tornadic debris signatures. [Available online at http://www.wdtb.noaa.gov/courses/dualpol/Applications/TDS/player.html.]

Rao, G. V., J. W. Scheck, R. Edwards, and J. T. Schaefer, 2005: Structures of mesocyclones producing tornadoes associated with tropical cyclone Frances (1998). *Pure Appl. Geophys.*, **162**, 1627–1641.

Schneider, D., and S. Sharp, 2007: Radar signatures of tropical cyclone tornadoes in central North Carolina. *Wea. Forecasting*, **22**, 278–286.

Ryzhkov, A. V., T. J. Schuur, D. W. Burgess, and D. S. Zrnić, 2005: Polarimetric tornado detection. *J. Appl. Meteor.*, **44**, 557–570.

Smith, B. T., R. L. Thompson, J. S. Grams, C. Broyles, and H. E. Brooks, 2012: Convective modes for significant severe thunderstorms in the contiguous United States. Part I: Storm classification and climatology. *Wea. Forecasting*, **27**, 1136–1153.

——, ——, A. R. Dean, and P. T. Marsh, 2015: Diagnosing the conditional probability of tornado damage rating using environmental and radar attributes. *Wea. Forecasting*, **30**, 914–932.

Snellman, L. W., 1982: Impact of AFOS on operational forecasting. Preprints, *Ninth Conf. on Weather Forecasting and Analysis*, Seattle, WA, Amer. Meteor. Soc., 13–16.

Spoden, P. J., R. A. Wolf, and L. R. Lemon, 2012: Operational uses of spectrum width. *Electronic J. Severe Storms Meteor.*, **7** (2), 1–28.

Spratt, S. M., D. W. Sharp, P. Welsh, A. C. Sandrik, F. Alsheimer, and C. Paxton, 1997: A WSR-88D assessment of tropical cyclone outer rainband tornadoes. *Wea. Forecasting*, **12**, 479–501.

Thompson, R. L., and M. D. Vescio, 1998. The destruction potential index—A method for comparing tornado days. Preprints, *19th Conf. on Severe Local Storms*, Minneapolis, MN, Amer. Meteor. Soc., 280–282.

——, B. T. Smith, J. S. Grams, A. R. Dean, and C. Broyles, 2012: Convective modes for significant severe thunderstorms in the contiguous United States. Part II: Supercell and QLCS tornado environments. *Wea. Forecasting*, **27**, 1136–1154.

Torres, S. M., and C. D. Curtis, 2007: Initial implementation of super-resolution data on the NEXRAD network. Preprints, *23rd Conf. on International Interactive Information and Processing Systems (IIPS) for Meteorology, Oceanography, and Hydrology*, San Antonio, TX, Amer. Meteor. Soc., 5B.10.

Verbout, S. M., D. M. Schultz, L. M. Leslie, H. E. Brooks, D. J. Karoly and K. L. Elmore, 2007: Tornado outbreaks associated with landfalling hurricanes in the North Atlantic Basin: 1954–2004. *Meteor. Atmos. Phys.*, **97**, 255–271.